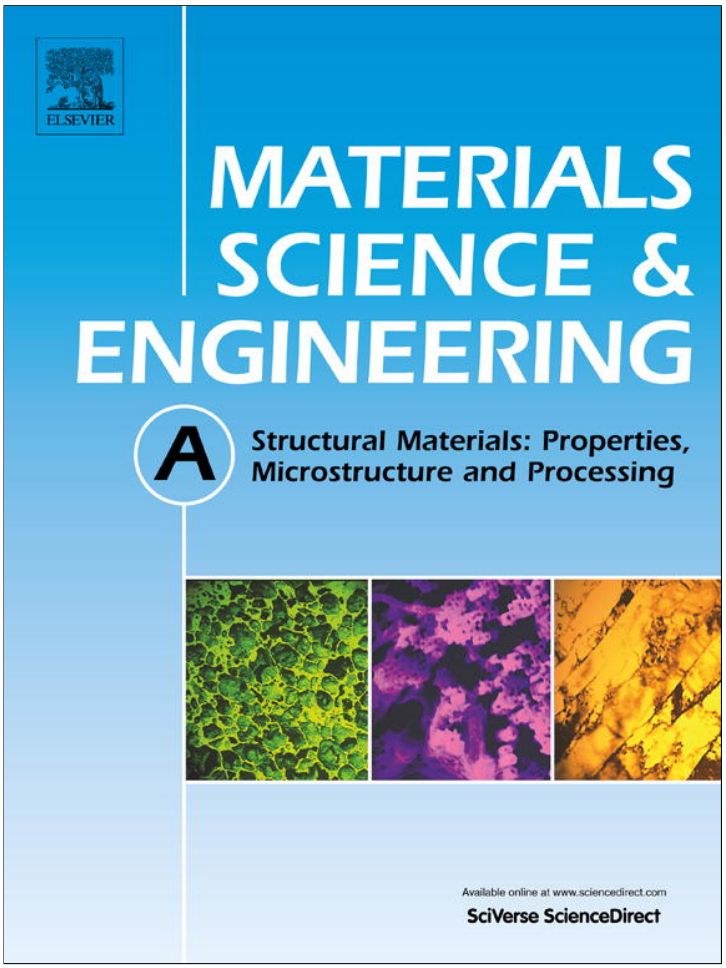

Materials Science & Engineering A 577 (2013) 16–22

Contents lists available at SciVerse ScienceDirect

Materials Science & Engineering A

journal homepage: www.elsevier.com/locate/msea

Effects of in situ formation of TiB_2 particles on age hardening behavior of Cu–1 wt% Ti–1 wt% TiB_2

Mohsen Sobhani [a,*], Alireza Mirhabibi [b], Hossein Arabi [a], R.M.D. Brydson [c]

[a] Center of Excellence for High Strength Alloys Technology (CEHSAT), School of Metallurgy and Materials Engineering, Iran University of Science and Technology, IUST, Tehran 16845-118, Iran
[b] Center of Excellence for Ceramic Materials in Energy and Environmental Applications(CECMEEA), IUST, Tehran 16845-118, Iran
[c] Institute for Materials Research, University of Leeds, Leeds LS2 9JT, United Kingdom

ARTICLE INFO

Article history:
Received 5 January 2013
Received in revised form
17 March 2013
Accepted 25 March 2013
Available online 3 April 2013

Keywords:
Cu–Ti
Age hardening
Composite
TiB_2
In situ

ABSTRACT

Age hardenable Cu–1 wt% Ti–1 wt% TiB_2 composite was produced by adding boron powder to Cu–Ti melt. TiB_2 nano-particles were formed via in situ reaction between titanium and boron in the melt. This composite was aged in a temperature range of 300–550 °C for a period of 1–25 h. Then, the age hardening behavior of the composite was compared with that of the binary Cu–2 wt% Ti alloy. The microstructure of the composite was examined with a high-resolution transmission electron microscope (HRTEM). The results of this study showed that TiB_2 particles can act as a heterogeneous nucleation site for β′(Cu_4Ti) precipitates. Substantial increase in tensile and yield stress of composite (i.e. 63% and 186% respectively) occurred relative to the solution state, after ageing at 450 °C for 10 h. The maximum strengthening of the composite was associated with precipitation of metastable Cu_4Ti near the ultra hard TiB_2 particles within the matrix. However, the results of this research show that the mechanical properties of aged composites are in good agreement with those of binary Cu–2 wt% Ti alloy; the maximum values of the hardness and electrical conductivity of the composite (i.e. 258 HV, 28% IACS) and the binary Cu–2 wt% Ti alloy (i.e. 264 HV, 17% IACS) were obtained when solution treated samples were aged at 450 °C for 10 h and 15 h, respectively.

1. Introduction

Copper and copper based alloys are widely used in numerous applications that require good mechanical properties along with good electrical conductivity. Age-hardenable copper–titanium alloys, containing approximately 1–5 wt% Ti, are capable of being a proper substitute for well-known Cu alloys, such as Cu–Be alloys. Formation of ordered metastable β′(Cu_4Ti) precipitates in Cu–Ti alloys during ageing increases their mechanical and electrical properties [1–3]. The mechanism of precipitation hardening in Cu–Ti binary alloys is a matter of much debate. It has been reported [4] that Cu–Ti alloys with Ti content less than 1 wt% decompose by nucleation and growth mechanism, while Cu–(2.5–5) wt% Ti exhibits spinodal decomposition during ageing [5].

Nagarjuna et al. [3] reported that Cu–Ti alloys having less than 1 wt% Ti are not suitable candidates for age hardening, since the amount of precipitated phase (Cu_4Ti) achievable by this amount of titanium during aging is very low and approaches zero in Cu–0.45 wt%Ti alloy. On the other hand, it has been reported [6] that by increasing Ti content, the electrical conductivity of copper matrix decreases dramatically, as the negative effect of Ti on electrical properties of copper alloys is more than that of the other common alloying elements such as Zn, Sn, and Ni. Therefore, in order to overcome this problem, some efforts have been made for modifying the precipitation behavior of Cu–Ti alloys via addition of other elements such as Co and Cr [7,8] or by aging in D_2 and H_2 atmospheres [1,9].

Among common reinforcing phases for copper matrix, addition of TiB_2 particles is well known for improving stiffness, hardness and mechanical strength of copper alloys. Moreover, the harmful effect of the dispersed TiB_2 particles on electrical conductivity of copper is much less than that of other ceramic reinforced particles [10–14]. Although there are some reports about the effect of TiB_2 particles on copper matrix strengthening via various methods such as powder metallurgy [11], melt mixing [12] and mechanical alloying [13], no reports have been published as yet about the effects of in situ formation of TiB_2 particles on age hardening behavior of Cu–Ti alloys. Therefore, the purpose of this investigation was a comparative study for the age hardening behavior, mechanical and electrical properties of Cu–1 wt% Ti–1 wt% TiB_2 composite and Cu–2 wt% Ti binary alloy.

* Correspondence to: P.O. Box 16845-118, Tehran, Iran. Tel.: +98 21 77459151; fax: +98 21 77240480.
E-mail address: m_sobhani@iust.ac.ir (M. Sobhani).

0921-5093/$ - see front matter © 2013 Elsevier B.V. All rights reserved.
http://dx.doi.org/10.1016/j.msea.2013.03.063

2. Experimental method

In the present study, Cu– 1 wt% Ti– 1 wt% TiB_2 in situ composite was prepared by melting together an appropriate amount of high purity copper (i.e. purity 99.99%) and 1.73 wt% titanium plate (i.e. purity 99.99%) in a vacuum induction melting (VIM) furnace. When the temperature of the melt reached 1200 °C and the vacuum became 3.5×10^{-2} mbar, 0.32 wt% boron powder encapsulated in a copper tube was charged into the melt. Then the melt was kept at 1200 °C for 15 min, allowing the melt to react completely with the boron powder. The melt was then cast into a low carbon steel mold fixed with a copper heat sink at its bottom. The quantitative chemical analysis of the ingot was conducted using inductively coupled plasma atomic emission spectroscopy (ICP-AES). The result of this analysis showed that the mean residual titanium content in the ingot was 0.94.%. Later the as-cast samples were rolled down to 60% of their thickness at room temperature. The rolled samples were homogenized for 20 h at 900 °C in an oxygen free molten salt bath that contained equal wt% of NaCl and $CaCO_3$ in order to avoid further oxidation and volatilization of the components. These samples were cooled to ambient temperature in air. The homogenized samples were subjected to solution treatment at 900 °C in the molten salt bath for 1 h and quenched in water in order to achieve a supersaturated solid solution. The quenched samples were aged in a temperature range of 300–550 °C for a period of 1–25 h and then quenched again in water.

Micro-harnesses of the samples were measured according to ASTM E384-99 standard with 50 g load. The flat type sub-size samples with dimensions of 25 mm gage length, 6 mm width and 1 mm thickness were made from cut strips of the samples according to ASTM E-8 standard. Tensile tests with cross head speed of 2 mm min^{-1} were conducted at room temperature. The electrical conductivity in % IACS (International Annealed Copper Standard) of samples was measured using a four-point probe method at room temperature according to ASTM B-193 standard. A scanning electron microscope (SEM) and a high-resolution transmission electron microscope (HRTEM) equipped with electron energy loss spectroscopy (EELS) were used for accurate detection of boron and light elements. In order to compare the effect of TiB_2 particles on age hardening, mechanical and electrical properties of the composite, a reference sample with Cu–2 wt% Ti composition was prepared in such a way that secondary elements in the matrix remained constant. The entire tests performed on the composite were also performed on this reference sample under the same conditions.

3. Results and discussion

BS-SEM micrograph in Fig. 1(a) shows the microstructure of Cu–1 wt% Ti–1 wt% TiB_2 composite after solidification. Formation of TiB_2 nano-particles within the matrix of composite can be clearly seen in this figure. Thermodynamically stable TiB_2 particles can be formed due to chemical reaction between elemental boron and titanium in molten copper [10–12]. As seen in this figure, TiB_2 particles formed in liquid copper had various sizes and irregular shapes. On average, the largest size of TiB_2 particles was about 2 μm and the smallest size was less than 100 nm. Based on previous research [10], TiB_2 particles size as well as their distribution is affected by many factors, including in situ reaction conditions, cooling rate and elements concentration. Since the melting point of boron (2092 °C) is higher than the melting temperature of copper (1083 °C), the boron powder should be chemically dissolved in molten copper, which is a time-consuming process. With increasing the solute concentration of boron in the melt, some boron element may be retained in the melt even after formation of many nano-TiB_2 particles. Hence, the extra dissolved boron in the molten copper having titanium element will be absorbed by primarily synthesized TiB_2 particles which leads to coarsening of smaller TiB_2 particles according to Gou et al. [10]. In other words, if both titanium and boron elements are consumed simultaneously within the melt, the TiB_2 nano-particles cannot be easily coarsened before solidification.

According to solid/liquid interface theories for MMCs [15,16], the distribution of TiB_2 particles is affected by solidification rate, density and wetting angle. In this regard, due to low wettability of TiB_2 particles by molten copper (i.e. wetting angle = 136°) [17], larger size TiB_2 particles are repulsed and redistributed toward the melting–freezing interfaces and finally to the grain boundaries, while nano size particles remained inside the grains. The microstructure of the composite after thermo-mechanical treatment (i.e. 60% reduction, homogenizing and solution treatment) is presented in Fig. 1(b). Due to relatively good distribution of nano-TiB_2 particles within the matrix in comparison to coarse TiB_2 particles, they were pinned to the new grain boundaries during recrystallization. A significant decrease in grain size with the presence of TiB_2 particles after recrystallization is shown in Figs. 1(b) and 2.

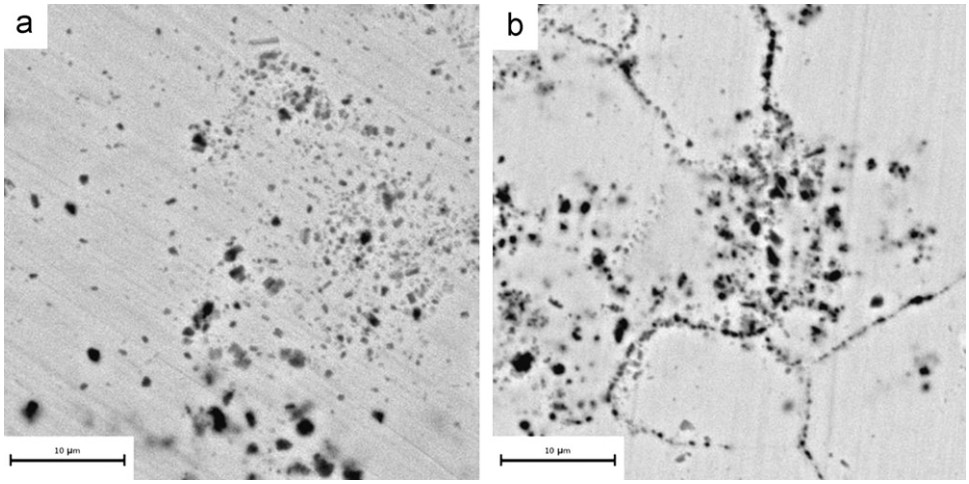

Fig. 1. BS-SEM micrograph of Cu–1 wt%Ti–1 wt%TiB_2 composite shows the distribution of TiB_2 particles within the matrix after (a) casting and (b) thermo-mechanical treatment.

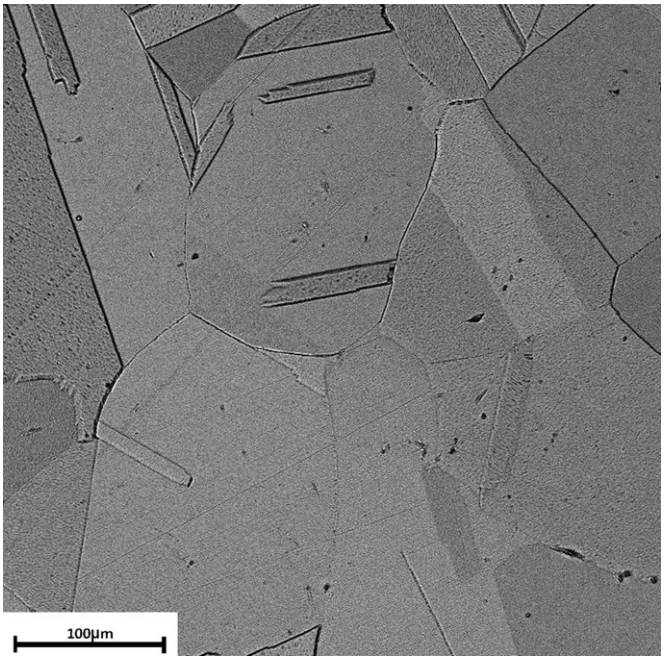

Fig. 2. Microstructure of Cu–2 wt% Ti after quenching from 900 °C.

This is in accordance with that of other researchers [18] who also reported that the presence of TiB_2 particles in grain boundaries could lead to a reduction in grain size and hinder grain growth at high temperature.

Typical TEM images (i.e. bright and dark field) of an as quenched composite with the selected area diffraction pattern (SADP) of TiB_2 particle are shown in Fig. 3. This figure shows that a large number of tangled dislocations were formed around TiB_2 particles. The difference between the thermal expansions of copper (16.6×10^{-6} 1/K) and TiB_2 particles (8.2×10^{-6} 1/K); leads to development of strain field at the interface between these particles and the copper matrix during quenching of the samples from solutionizing temperature to ambient temperature. This thermal strain can cause punching dislocations from the interface of TiB_2 particles out into the matrix. These dislocations and other structural defects can increase the diffusion rate of titanium required for formation Cu_4Ti and might be appropriate nucleation sites for heterogeneous precipitation of transitional β′(Cu_4Ti) phase in the matrix according to Dutkiewicz [19].

Fig. 4 shows the typical HRTEM image of the as quenched composite after being re-solutionized at 900 °C for 10 min. HRTEM image together with the map of elements via EELS indicates that there are a fair amount of TiB_2 particles formed within the matrix. As seen in this figure, titanium concentration in the vicinity of TiB_2 particles increased substantially. This means the localized diffusion rate near these particles was more than that of the bulk of material due to increase of dislocation density around these particles during heat treatment (i.e. dislocation punch-up) as shown in Fig. 3(a). This can increase the possibility of formation of Cu_4Ti precipitates near TiB_2 particles during aging. However, when the composite solutionized at 900 °C for 1 h and aged at 450 °C for 10 h a large amount of β′ (Cu_4Ti) precipitates was formed near TiB_2 particles within the matrix. HRTEM micrographs of composite at peak aged (maximum hardness) condition (i.e. 10 h –450 °C) with selected area diffraction (SAD) pattern of β′ and FFT pattern of TiB_2 particle are shown in Fig. 5. This figure is a clear evidence that a large amount of β′(Cu_4Ti) precipitate as formed in the vicinity of TiB_2 particle within the matrix. This is an indication of higher diffusion rate of titanium in the region near the TiB_2 particles as this region has high dislocation density, as referred to earlier. It should be mentioned that due to heterogeneity of TiB_2 distribution, the distribution of β′ phase was also non-homogeneous. This phenomenon confirms that the region having higher dislocation density has a greater effect on the formation of β′ phase. SAD pattern of β′ precipitates has been presented in Fig. 5 (c). This figure confirms that the particles nucleated near TiB_2 particles are β′(Cu_4Ti) as their crystal structure is tetragonal with lattice parameters of $a=0.584$ nm and $c=0.362$ nm. Unlike the irregular shape of TiB_2 particles, the Cu_4Ti has spherical shape with a mean size under 10 nm. It is worth mentioning that both needle and spherical shapes have been reported by other researchers [9,20,4] for β′(Cu_4Ti) precipitates. Fig. 5(b) shows the growth of β′ precipitates within the matrix after formation, as the larger particles may indicate a nucleation and growth mechanism for formation of β′ precipitate according to Borchers [4].

Fig. 6 shows the variation of hardness of Cu–1 wt% Ti–1 wt% TiB_2 composite and Cu–2 wt% Ti alloy as a function of ageing time. The hardness of the as quenched Cu–1 wt% Ti–1 wt% TiB_2 (i.e. 115 HV) was higher than that of the as quenched Cu–2 wt% Ti alloy (i.e. 90 HV). The higher hardness of the composite compared with that of Cu–2 wt% Ti alloy after quenching was attributed to the presence of TiB_2 particles, higher dislocation density around TiB_2 particles and according to the Hall–Petch model, to smaller grain size (Figs. 1 and 2).

Ageing curve of the composite in Fig. 6(b) shows that the least hardness was achieved at 300 °C for all ageing times relative to the other temperatures (400–450–550 °C). At this temperature, hardness decreased in the first 2 h of ageing and then rose with further ageing time. Thompson and Williams [21] reported similar observation for Cu–2.5 wt% Ti alloy. This phenomenon can be explained by considering a) climb and glide of dislocations in the matrix and b) nucleation, coarsening and dissolution of precipitates phase. At 300 °C, before formation of a considerable amount of β′, some punch out dislocations, emitted from the TiB_2 interface within the matrix were annihilated by climb mechanism. This leads to relaxation of the interfacial stress and therefore causes to drop in hardness of composite in the initial stage of ageing. In addition, the diffusion rate of titanium within the matrix during ageing can declineby the decrease in dislocation density which causes a delay in precipitation of β′. Thus, one may conclude that 300 °C is not enough to provide

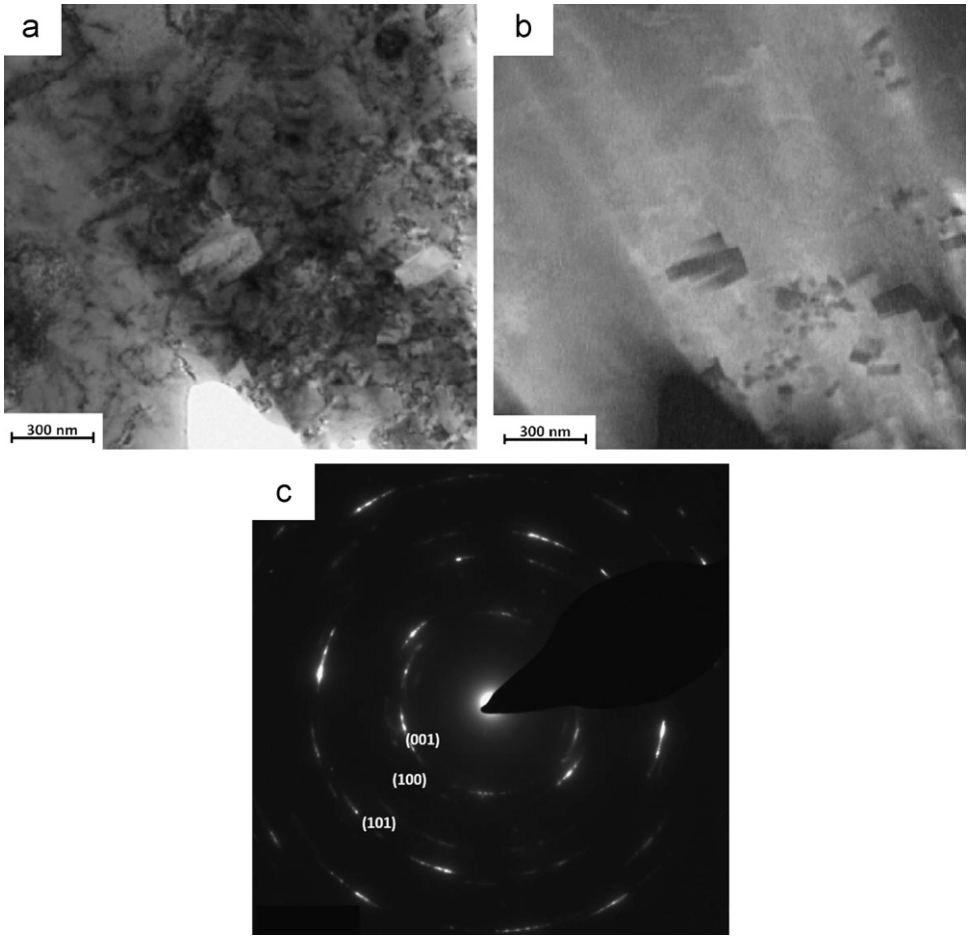

Fig. 3. (a) Bright field TEM image shows the formation of tangled dislocations in the vicinity of TiB_2 particles after quenching, (b) dark field and (c) SAD pattern of TiB_2 particle.

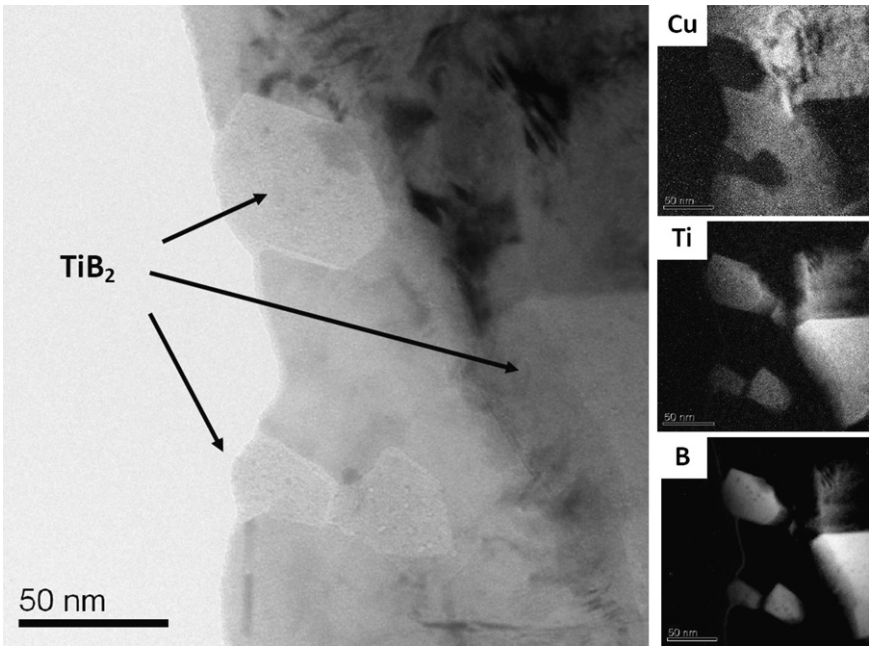

Fig. 4. HRTEM image of the re-solutionized and quenched Cu–1 wt%Ti–1 wt%TiB_2 with dot point elements maps.

sufficient energy for higher rates of titanium diffusion that is required for formation of Cu_4Ti. On the other hand, according to Bozic et al. [20], as the motion of a pair of super-dislocations is strongly dependent on the statistical configuration of obstacles present in the system, the structural ordering in titanium rich region and disappearance of anti-phase boundary during the initial stage of

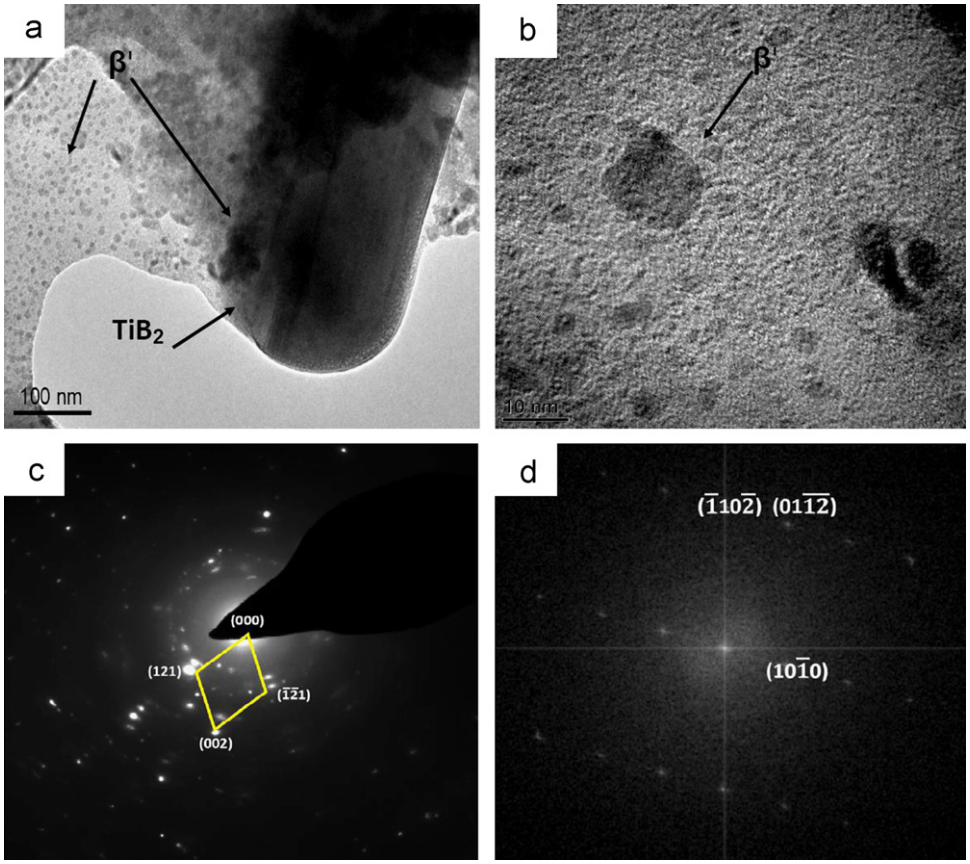

Fig. 5. HRTEM micrograph of Cu–1 wt% Ti–1 wt% TiB_2 aged at 450 °C for 10 h (a) β′(Cu_4Ti) formed near TiB_2 particle, (b) β′ growth, (c) SAD pattern of β′(Cu_4Ti) and (d) TiB_2 FFT pattern.

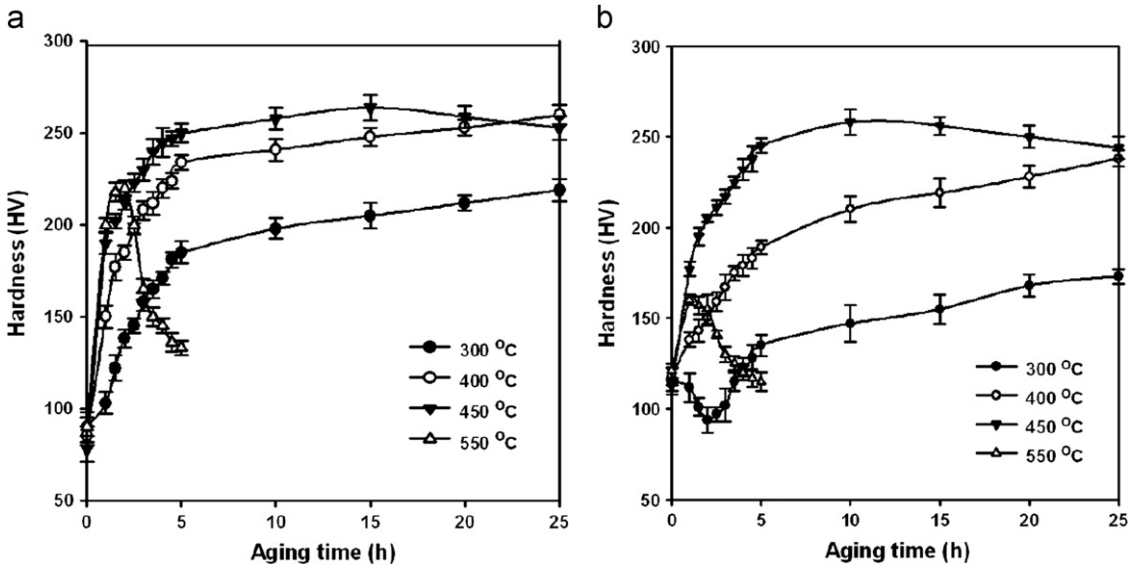

Fig. 6. Variation of hardness as a function of ageing time for different temperatures. (a) Cu–2 wt% Ti and (b) Cu–1%wtTi–1%wtTiB_2.

ageing, can result in eased dislocation motion. As a result, the hardness decreases in the first 2 h of the ageing. Then with further ageing time, the hardness of the composite can increase due to the formation of metastable precipitation of Cu_4Ti (β′) in the matrix.

Harnesses of composite and binary alloy are increased with increasing ageing time at 400 °C. However, both of them have not attained peak hardness even after 25 h ageing at this temperature. The volume fraction of β′-Cu_4Ti precipitate increases considerably with Ti content as well as ageing time according to lever rule in Cu–Ti phase diagram (Fig. 7). Therefore, the amount of precipitates phase of β′ which formed during ageing in binary alloy is higher than that for composite sample; hence the hardness of the binary alloy is higher than that of the composite.

Variation of hardness with ageing time at 550 °C is presented in Fig. 6(a) and (b). This figure shows that hardness increases in the first 2 h of ageing. This is in agreement with reported work of Datta and Soffa [22], who attributed the increase in hardness to formation of ordered metastable and coherent β′(Cu_4Ti) phase

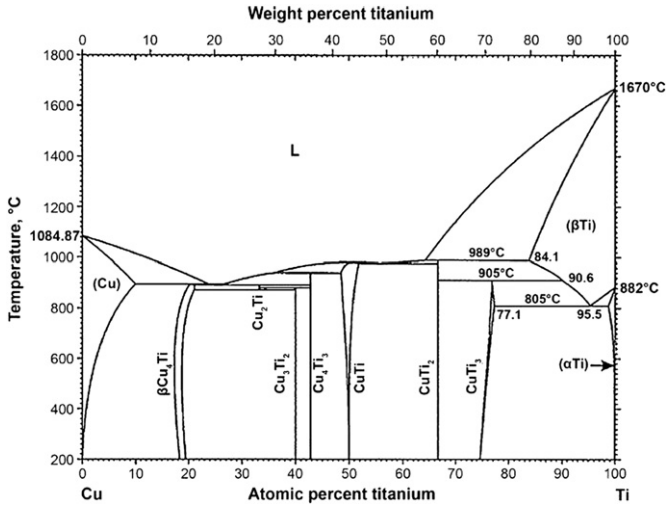

Fig. 7. Cu-Ti binary phase diagram.

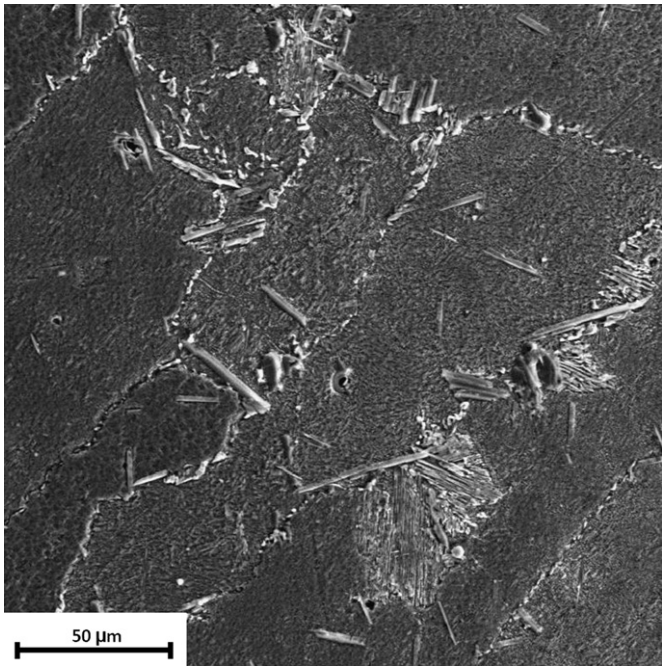

Fig. 8. Microstructure of Cu–2 wt% Ti binary alloy after 25 h aging at 450 °C shows formation of cellular type precipitate at grain boundaries.

within the matrix. However, the decrease in hardness after 2 h of ageing at 550 °C can be due to polymorphic transformation of β′ (Cu_4Ti) (tetragonal) to β′(Cu_4Ti) (orthorhombic) and also precipitates growth according to Soffa and Laughlinb [2]. In addition, based on Cu–Ti phase diagram (Fig. 7), this temperature was very close to the solvus temperature of the composite having 1 wt% Ti against 2 wt% Ti in the binary alloy. Therefore, one may conclude that ageing of composite at this temperature leads to a faster dissolution and/or overageing of precipitate phase in the composite than the binary alloy, resulting in higher reduction in hardness after 2 h of ageing at 550 °C. It can also be seen that the maximum hardness of the composite at this condition is lower than that of the binary alloy, which in turn is due to the formation of a lower amount of precipitate phase within the composite in comparison to that of the binary alloy, as mentioned earlier.

The effective factors on hardness (i.e. dislocation elimination and formation of precipitate) change in such a way as to cause higher ageing kinetics at 450 °C. In the absence of TiB_2 particles, the maximum hardness of Cu–2 wt% Ti alloy (i.e. 264 HV) occurred after 15 h while the maximum hardness of the composite (i.e. 258 HV) was achieved after 10 h ageing at 450 °C. The increase in ageing kinetics of the composite in the presence of TiB_2 particles can be attributed to nucleation of β′ precipitates on basal plane of TiB_2 particles which basically occurs in the vicinity of TiB_2 particles,as shown in Fig. 5(a). The rate of decrease in hardness after passing the peak value in the composite (i.e. 0.9 HV/h) is less than that of Cu–2 wt % Ti alloy (i.e. 1.1 HV/h). This behavior can be explained by considering the retarding influence of TiB_2 particles on the coarsening of larger number of metastable Cu_4Ti particles according to Bozic et al. [20]. On the other hand, according to a similar research by Cornie et al. [23], the decrease in hardness value of Cu–2 wt% Ti alloy after peak aged condition can be due to the formation of cellular (discontinues) precipitates at the grain boundaries, see Fig. 8.

Hardness, tensile properties and electrical conductivity of the as cast, as quenched and peak-aged composites were measured and are presented in Table 1, together with similar properties of Cu–2 wt% Ti binary alloy. The results show a considerable increase in electrical conductivity of peak aged (i.e. 28% IACS) composite relative to as cast (8% IACS) and as quenched (15% IACS) conditions. This increase in electrical conductivity can be attributed to the formation of β′ precipitate within the matrix according to Nagarjuna et al. [6]. These researchers state that an increase in resistivity due to the increasing volume fraction of Cu_4Ti precipitate is lower than the amount of decrease in resistivity due to removal of Ti from the matrix, thereby resulting in an overall increase in electrical conductivity in peak-age composite in comparison to the solution treated one. As seen in this table, the electrical conductivity of composite at peak aged condition is 65% higher than that of the binary Cu–2 wt% Ti alloy. The higher electrical conductivity observed in composite was analyzed by considering the interaction between conductive electrons and reinforced particles. In this regard, two effective factors can be considered in evaluating the electrical conductivity of copper matrix. These are resistivity of the particles and scattering surface of conductive electrons. In other words, as the electrical resistivity of TiB_2 particles (i.e. 6.6 μΩ cm) [24] is less than that of Cu_4Ti precipitate (i.e. 38.5 μΩ cm) [6], the detrimental effect of TiB_2 particles on electrical conductivity of copper must be lower than that of Cu_4Ti precipitates. On the other hand, as mentioned previously, the amount of Cu_4Ti precipitate in the composite even at peak-aged condition is less than that of the binary alloy. This together with the fact that Cu_4Ti particles precipitate in the vicinity of TiB_2 particles (Fig. 5) can cause a reduction in scattering surface of the conductive electrons. In other words, the scattering surface of the conductive electrons due to formation of β′ precipitates in composite did not rise much during the ageing process in comparison to the binary alloy. Consequently, the electrical conductivity of composite increases more than that of binary alloy during ageing according to Nordheim's rule [6,3].

Table 1 shows a substantial increase in tensile properties of the sample under peak-aged condition when compared with those of the as quenched sample. The increases in yield and tensile strength of peak-aged composite sample relative to the as quenched sample are 270 MPa and 228 MPa respectively, while those increase for the Cu–2 wt% Ti binary alloy are 232 MPa and 197 MPa respectively. The increases in the ultimate and yield strengths of composite during ageing were higher than those of binary Cu–2 wt% Ti alloy. Therefore, one may conclude that the mechanism of strain hardening in the composite having both non-shearable TiB_2 particles and shearable β′(Cu_4Ti) particles was different from the mechanism of strain hardening of Cu–2 wt% Ti

Table 1
Comparison of properties of Cu–1 wt% Ti–1 wt%TiB_2 composite with those of Cu–2 wt% Ti alloy.

Property	Cu–1 wt%Ti–1 wt% TiB_2			Cu–2 wt% Ti		
	As cast	As quenched	Peak age (10hrs–450 °C)	As cast	As quenched	Peak age (15hrs–450 °C)
%IACS	8	15	28	7	8	17
Hardness (HV)	85	115	258	115	90	264
YS (MPa)	–	145	415	–	185	417
UTS (MPa)	–	362	590	–	418	615
El (%)	–	32	21	–	38	24

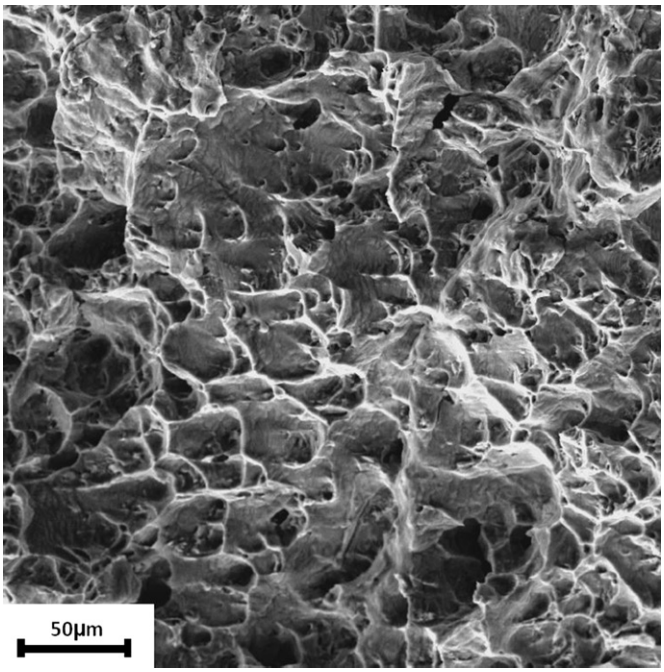

Fig. 9. Fracture surface of Cu–1 wt% Ti–1 wt% TiB_2 composite after 10 h aging at 450 °C.

alloy without any non-shearable strengthening particles. In other words, in the composite, both shearable and non-shearable particles can slow down dislocation movement leading to high strength, while in Cu–2 wt% Ti alloy only the shearable β′ (Cu_4Ti) particles effect the strengthening of the alloy. This means that consecutive passes of dislocation through these particles decrease, so the required force for movement of dislocation through these particles gradually decreases. The ductility of composite (%EL=21) is slightly less than that of Cu–2 wt% Ti alloy (%EL=24) under peak aged condition. This was attributed to the presence of ultra-hard TiB_2 particles in the matrix of composite which lowered the dislocation movement, and hence lowered ductility. Nevertheless one should note that the dimple characteristic of the fracture surface of the composite (Fig. 9) indicates a ductile mode of fracture in the composite which means TiB_2 nano-particles did not affect the mode of fracture despite their ultra-hardness.

4. Conclusions

1. In situ formation of TiB_2 in Cu–1 wt% Ti–1 wt% TiB_2 composite makes it possible to access a favorable combination of high hardness and electrical conductivity after ageing treatment.
2. HRTEM analysis of Cu–1 wt% Ti–1 wt% TiB_2 composite confirmed the presence of metastable β′(Cu_4Ti) precipitates formed near the TiB_2 particles when aged at 450 °C for 10 h.
3. Cu_4Ti reinforcing particles initially precipitate near TiB_2 particles possibly due to the presence of punched out dislocations around the TiB_2 particles. This caused heterogeneous nucleation sites for formation of Cu_4Ti precipitates.
4. Ductile mode of fracture was observed in Cu–1 wt% Ti–1 wt% TiB_2 composite at peak aged condition.
5. The electrical conductivity of the composite increased due to formation of metastable precipitates (β′) in the matrix and reached 28% IACS after 10 h of aging at 450 °C.
6. The maximum hardness, yield and ultimate tensile strengths of the composite (258 HV, 415 MPa, 590 MPa; respectively) were achieved after 10 h while the maximum mechanical properties of Cu–2 wt% Ti alloy (264 HV, 417 MPa, 615 MPa; respectively) were achieved after 15 h of ageing at 450 °C.

Acknowledgment

The authors are grateful to professor R.M.D. Brydson, Department of School of Process, Environmental and Materials Engineering, University of Leeds, for providing TEM facility in Leeds Electron Microscopy and Spectroscopy Centre. The authors would like to express their gratitude to the Iranian Nanotechnology Initiative for financially supporting this project.

References

[1] S. Semboshi, T. Al-Kassab, R. Gemmab, R. Kirchheim, Ultramicroscopy 109 (2009) 593–598.
[2] W.A. Soffa, D.E. Laughlinb, Prog. Mater. Sci. 49 (2004) 347–366.
[3] S. Nagarjuna, M. Srinivas, K. Balasubramanian, D.S. Sarma, Mater. Sci. Eng. A 259 (1999) 34–42.
[4] C. Borchers, Philos. Mag. A 79-3 (1999) 537–547.
[5] I.S. Batra, G.K. Dey, U.D. Kulkarni, S. Banerjee, Mater. Sci. Eng. A 360 (2003) 220–227.
[6] S. Nagarjuna, K. Balasubramanian, D.S. Sarma, Mater. Sci. Eng. A 225 (1997) 118–124.
[7] S. Nagarjuna, K.K. Sharma, I. Sudhakar, D.S. Sarma, Mater. Sci. Eng. A 313 (2001) 251–260.
[8] R. Markandeya, S. Nagarjuna, D.S. Sarma, Mater. Charact. 57 (2006) 348–357.
[9] S. Semboshi, T. Nishida, H. Numakura, T. Al-Kassab, R. Kirchheim., Metall. Mater. Trans. A 42A (2011) 2136–2143.
[10] M. Guo, K. Shen, M. Wang, Acta Mater. 57 (2009) 4568–4579.
[11] S. Dallaire, J.G. Legoux, Mater. Sci. Eng. A 183 (1994) 139–144.
[12] J.H. Kim, J.H. Yun, Y.H. Park, K.M. Choa, I.D. Choi, I.M. Park, Mater. Sci. Eng. A 449–451 (2007) 1018–1021.
[13] S.J. Dong, Y. Zhou, Y.W. SHI, B.H. Chang, Metall. Mater. Trans. A 33A (2002) 1275–1280.
[14] P. Yid, D.D.L. Chung, J. Mater. Sci. 32 (1997) 1703–1709.
[15] D. Shangguan, S. Ahuja, D.M. Stefanescu, Metall. Mater. Trans. A 23 (1992) 669–680.
[16] D.M. Stefanescu, B.K. Dhindaw, S.A. Kacar, A. Moitra, Metall. Mater. Trans. A 19 (1988) 2847–2855.
[17] G.A. Yasinskaya, Powder Metall. Met. Ceram. 5-7 (1966) 557–559.
[18] Z.Y. Ma, S.C. Tjong, Mater. Sci. Eng. A 248 (2000) 70–76.
[19] J. Dutkiewicz, Metall. Mater. Trans. A 8 (1977) 751–761.
[20] D. Bozic, J. Stasic, J. Ruzic, M. Vilotijevic, V. Rajkovic, Mater. Sci. Eng. A 528 (2011) 8139–8144.
[21] A.W. Thompson, J.C. Williams, Metall. Mater. Trans. A 24 (1984) 931–937.
[22] A. Datta, W.A. Soffa, Acta Metall 124 (1976) 987–1001.
[23] J.R. Cornie, A. Datta, W.A. Soffa, Metall. Mater. Trans. A 4 (1973) 727–733.
[24] F.W. Vahldiek, J. Alloys Compd. 3 (1976) 202–209.